



ORIGINAL ARTICLE

A combined computational & electrochemical exploration of the *Ammi visnaga* L. extract as a green corrosion inhibitor for carbon steel in HCl solution



Aouatife Zaher^a, Ruby Aslam^b, Han-Seung Lee^{c,*}, Azzeddine Khafouri^d, Moncef Boufellous^a, Awad A. Alrashdi^e, Yasmina El aoufir^f, Hassane Lgaz^{c,*}, Mohammed Ouhssine^a

^a Laboratory of Natural Resources and Sustainable Development, Biology Department, PB 133-14050, Kenitra, Morocco

^b Corrosion Research Laboratory, Department of Applied Chemistry, Faculty of Engineering and Technology, Aligarh Muslim University, Aligarh 202002, India

^c Department of Architectural Engineering, Hanyang University-ERICA, 1271 Sa 3-dong, Sangrok-gu, Ansan 426791, Republic of Korea

^d Laboratory of Geoheritage, Geoenvironment and Prospecting of Mines & Water, Faculty of Sciences, Mohammed Premier University, Oujda, Morocco

^e Chemistry Department, Umm Al-Qura University, Al-Qunfudah University College, Saudi Arabia

^f Laboratoire de Chimie organique, Catalyse et Environnement, Ecole supérieure d'éducation et de la formation, Ibn Tofail University, PB 133-14050 Kenitra, Morocco

Received 4 October 2021; accepted 14 November 2021

Available online 19 November 2021

KEYWORDS

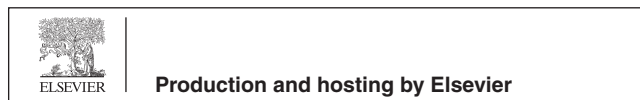
Corrosion inhibition;
Green inhibitor;
Carbon steel;
Ammi visnaga;
DFT;
Molecular dynamics

Abstract Natural-based corrosion inhibitors have gained great research interest thanks to their low cost and higher performance. In this work, the chemical composition of the methanolic extract of *Ammi visnaga* umbels (AVU) was evaluated by gas chromatography (GC) coupled with mass spectrometry (MS) and applied for corrosion inhibition of carbon steel (CS) in 1.0 mol/L HCl using chemical and electrochemical techniques along with scanning electron microscope (SEM) and theoretical calculations. A total of 46 compounds were identified, representing 89.89% of the overall chemical composition of AVU extract, including Edulisin III (72.88%), Binapacryl (4.32%), Khellin (1.97%), and Visnagin (1.65%). Chemical (Weight loss) and electrochemical (potentiody-

* Corresponding authors.

E-mail addresses: ercleehs@hanyang.ac.kr (H.-S. Lee), hlgaz@hanyang.ac.kr (H. Lgaz).

Peer review under responsibility of King Saud University.



dynamic polarization curves (PPC), and electrochemical impedance spectroscopy (EIS)) techniques revealed that investigated extract can be used as an effective corrosion inhibitor for carbon steel in 1.0 mol/L HCl solution. At a low dose of 700 ppm, the inhibitory action of AVU extract reached an inhibition efficiency of 84 percent. According to polarization tests, the investigated extract worked as a mixed inhibitor, protecting cathodic and anodic corrosion reactions. The EIS test showed that upon the addition of AVU extract to HCl solution, the polarization resistance increased while the double layer decreased. SEM images showed a protected CS surface in the inhibited solution. Quantum chemical calculations by Density Functional Theory (DFT) for the main components confirmed the major role of heteroatoms and aromatic rings as adsorption sites. Molecular dynamics (MD) simulation was used to study the adsorption configuration of the main components on the Fe(110) surface. Outcomes from this study further confirmed the significant advantage of using plant-based corrosion inhibitors for protecting metals and alloys.

© 2021 The Authors. Published by Elsevier B.V. on behalf of King Saud University. This is an open access article under the CC BY-NC-ND license (<http://creativecommons.org/licenses/by-nc-nd/4.0/>).

1. Introduction

Corrosion is a thermodynamically spontaneous process that involves the chemical or electrochemical interaction of metals or alloys with the surrounding constituents, resulting in the change of metals or alloys to a more stable state (Jafari et al., 2019; Laamari et al., 2011). The negative consequences of corrosion significantly impact metallic structures, maintenance costs, and public welfare. The approximated global cost of corrosion is \$2.5 trillion (USD), which is around 3.4% of industrialized nations' Gross Domestic Product (GDP). Some 15% (\$ US 375 billion) – 35% (\$ US 875 billion) range of this cost can be neglected by accomplishing felicitous corrosion prevention tactics (Koch et al., 2016). Carbon steel is one of the preferred engineering materials in the industrial arena, including oil and gas transportation pipelines, downhole casing, reinforced concrete, vehicles, refining, and chemical processing, despite its non-corrosion resistance, particularly in acidic circumstances (Mobin et al., 2017). Carbon steel is a significant building component because of its exceptional mechanical properties and low cost. On the other hand, pickling, acid cleaning of boilers, descaling, oil well acidizing, and other industrial applications of acidic solutions are routinely used to remove deposited rust, iron oxide scale for enhancing oil production (Khalaf et al., 2020). The most often used corrosive acids during such processes are hydrochloric acid and sulphuric acid (Aourabi et al., 2020; Hemapriya et al., 2020; Lgaz et al., 2020a).

The addition of corrosion inhibitors to acidic solutions is the first choice to reduce their aggressiveness and thus the corrosion rate. Inhibitors with electronegative elements including O, S, N, P, conjugation, double or triple bonds, and aromatic rings provide greater corrosion mitigation (Verma et al., 2021). These compounds work by adsorbing onto the surface of a metal substrate and producing a protective layer, making it impervious to the harsh external environment. The degree of corrosion protection provided by an inhibitor is, in most cases, proportional to its concentration and depends on its physico-chemical properties (Verma et al., 2018c). It has been reported in many studies that increasing the inhibitor concentration increases fractional surface coverage by an extra number of inhibitor molecules, which may be limited to a fixed optimal concentration due to surface saturation (Mobin et al., 2020).

The use of harmful synthetic inhibitors, especially inorganic ones, is no longer permitted due to increased environmental awareness. As a result, current research focuses on non-hazardous, biodegradable, less expensive, and ecologically friendly corrosion inhibitors. Plant extracts represent a plentiful category of corrosion inhibitors as most of these materials are easily obtainable and non-poisonous (Saxena et al., 2018). Many studies examining plant extracts have revealed that various extracts of leaf, root, bark, stem, pulp, and fruit are being investigated as corrosion inhibitors for various metals and alloys (Verma et al., 2018a). Plant extracts such as *Eucalyptus* leaves (Dehghani et al., 2019a), *Primula vulgaris* flower extract (Majd et al., 2019) *Aloe vera* (Abiola and James, 2010), ginger (Gadow and Motawea, 2017; Liu et al., 2019), turmeric rhizomes (Al-Fakih et al., 2015), olives leaf (Harb et al., 2020), olive roots, stems, and leaves (Bouknana et al., 2015), *Mentha rotundifolia* leaves (Khadraoui et al., 2014), *Jathropa* leaf (Ikpeseni et al., 2021), *Cashew nut* sheel (Furtado et al., 2019), *Hibiscus* leaf extract (Hoai et al., 2019), *Coriandrum Sativum* L. Seeds Extract (Kadiri et al., 2018) Henna Extract (Fouda et al., 2019), *Amaranthus* (Srivastava, 2020), *Myrmecodia pendans* Extract (Pradityana et al., 2016), Castor oil (Farhadian et al., 2020), binary mixture of sesame and castor oil (Oyekunle et al., 2019), *Azadirachta indica* (Sharma et al., 2015), neem (Sharma et al., 2009), *Halopitys Incurvus* Extract (Benabbouha et al., 2018), potato (Shekhar et al., 2021), *Lagerstroemia speciosa* leaf extract (Mobin et al., 2019b) and pineapple stem extract (Mobin et al., 2019a) among others have been investigated as good corrosion inhibitors. Experiments were carried out in acidic, alkaline, and neutral environments to test their corrosion inhibition performance for various ferrous and non-ferrous alloys. Polyphenolic secondary metabolites, such as flavonoids, tannins, resveratrol tannin, and coumarin, gallic acid, sterols, alkaloid berberine pyrrolidine, ascorbic acids, amino acids, and carotene, are among the main constituents found in these plants. The corrosion inhibition effect is due mainly to synergistic adsorption of different components or those with a higher percentage.

Ammi visnaga (Khella) belongs to the *Apiaceae/Umbelliferae* family. It is an annual herbaceous folk plant that grows wild in the Mediterranean area, particularly in Egypt, Morocco, and the Islamic Republic of Iran, with bi- or tripinatisect linear segmented leaves and huge compound umbels of white

flowers. It is referred to as “Bechnikha” in the local Moroccan dialect. This is an important part of the local floristic history (Chraka et al., 2020). The literature review reveals that *Ammi visnaga* has been used to treat psoriasis, asthma, vitiligo recovery, hypoglycemia, and toxic bites (Bhagavathula et al., 2015). Many common drugs have been developed from khella, including amiodarone, nifedipine, and cromolyn. The ability of *Ammi visnaga* seeds to reduce carbon steel corrosion in the acidic medium (Zaher et al., 2020) and the essential oil of the plant to prevent brass corrosion in NaCl media (Chraka et al., 2020) has been documented.

In light of these facts, herein, the methanolic extract of *Ammi visnaga* dry umbels was chosen to study its anti-corrosive performance for carbon steel in 1 mol/L HCl medium by employing weight loss measurements, electrochemical impedance spectroscopy, potentiodynamic polarization curves coupled with surface characterization by scanning electron microscope (SEM). The principal constituents prevailing in AVU extract were identified utilizing GC/MS. It should be noted here that for the well acidization process, which is a maintenance technique to remove mineral deposits from wells, a high HCl concentration ranging from 15 to 20 wt% is used (Reynolds, 2020). To limit the corrosion effect on equipment, a corrosion inhibitor formulation (CIF) composed of inhibitor molecules, intensifiers, surfactants, metal chelating agents is added to HCl solution (Brezinski, 1999; Reynolds, 2020). Bearing this in mind, the present work is a contribution to investigate the corrosion inhibiting properties of AVU extract, and therefore its potential incorporation into a CIF. The 1.0 mol/L HCl is selected as a reference for laboratory tests.

Furthermore, considering the presence of several compounds, theoretical investigation of the major components can provide useful insights into their electronic properties. Therefore, the active sites are responsible for interacting with the metal surface (Bahlakeh et al., 2019a; Dehghani et al., 2019b, 2020b, 2020c). These insights can be achieved by implementing DFT calculations of selected components. In addition, molecular dynamics simulation is an interesting choice for studying the adsorption of major components on the metal surface. Taking these into consideration, these theoretical tools are used in the present work to investigate the adsorption behavior of AVU extract's components on the steel surface.

2. Material and methods

2.1. Collection and preparation of methanolic extract

The plant was collected in October 2015 in the Sidi Slimane region of Morocco, a rural section of the Rabat-Salé-Kenitra area. *Ammi visnaga* umbels were crushed and ground into a fine powder. Soxhlet extraction with methanol was performed (Jensen, 2007). To this end, 15 g of the powder was put in a cartridge, and 300 mL of solvent (99.8% methanol) was used to extract it. The extraction process was continued until the solvent retrieved was colorless (6 h). The solvent rich in extracted compounds was collected in a flask, then allowed to evaporate completely in a rotary evaporator at mild temperature (40 °C) to remove the solvent, after which it was weighed. The extraction yield was 18.2%. The resulting extract was kept at 4 °C.

2.2. Chromatographic characterization

The chromatographic analysis of the methanolic extract of *Ammi visnaga* umbels was carried out using a Bruker 456 GC Triple Quadrupole EVOQ gas chromatography-mass spectrometer equipped with an 8400 series auto-injector (Bruker, Germany). The system was equipped with an RXI-5SIL MS column (30 m × 0.25 mm × 0.25 μm film thickness, Bruker, Germany). The temperature was set from 35 °C to 300 °C at 5 °C min⁻¹ and then held at 300 °C for 10 min. Helium gas was used as a carrier gas with a constant flow rate of 1.5 mL min⁻¹. A 1.0 μl of samples were automatically injected into the non-split mode. The temperature of the mass spectrometry interface was 280 °C. For CG mass detection, an electron ionization system with ionization energy of 70 eV was used and the scanning range was 10–600 amu. The identification and percentage composition of the compounds were performed using the mass spectrometry library and the NIST 2014, 11th Edition and WILEY 5th Edition spectrometer data bank.

2.3. Corrosion tests

2.3.1. Carbon steel specimens and aggressive solution

Carbon steel was employed as the working electrode in this investigation, and its chemical and mass composition are: 0.370% C, 0.230% Si, 0.680% Mn, 0.016% S, 0.077% Cr, 0.011% Ti, 0.059% Ni, 0.009% Co, 0.160% Cu, and balance Fe. A clean surface condition is required for optimum measurement reliability. The samples' surfaces were mechanically polished using abrasive papers (carbon, silica) with increasing particle sizes ranging from 80 to 1200 mm, then rinsed with distilled water, acetone and dried. The corrosive solution (1.0 mol/L) was made with bidistilled water from a concentrated 37% HCl solution. Pre-trial tests were carried out to select the appropriate concentration range, which is fixed between 150 and 700 ppm of AVU extract.

2.3.2. Gravimetric measurements

Gravimetric experiments were performed to determine the concentration impact of AVU extract on carbon steel corrosion at different temperatures (303 to 333 K). The carbon steel specimens were immersed in 1.0 mol/L HCl for 12 h, according to the ASTM G1-90 designation (Metals, 2017). The experiments were conducted in a double-walled cell with a condenser and a thermometer. The electrolyte was kept at the desired temperature by a circulating water thermostat. The specimens were immersed in 250 mL beaker containing the 250 mL electrolyte. After the immersion, the carbon steel specimens were completely cleaned with demineralized water and gently scrubbed with a bristle brush to eliminate the corrosion products. They were then cleaned with acetone and twice distilled water. Finally, the test specimens were dried to check that their weight remained consistent. Each gravimetric test value is the average of three tests. The corrosion rate and inhibition efficiency (η_w %) can be calculated by using Eq. (1) and Eq. (2), respectively:

$$v = \frac{w_1 - w_2}{AT} \quad (1)$$

$$\eta_w = \frac{v_o - v_i}{v_o} \times 100 \quad (2)$$

where w_1 and w_2 are the weight of the specimen before and after immersion, A is the surface area of the carbon steel specimen (cm^2); and T is the exposure time (h), v_o and v_i are the corrosion rates in the absence and presence of AVU extract, respectively.

2.3.3. Electrochemical studies

PGZ 301 Potentiostat/Galvanostat controlled by Volatamaster 4 software package was used to perform all electrochemical measurements. A conventional three-electrodes cell was used consisting of the CS serves as the working electrode, saturated calomel electrode (SCE) as the reference electrode, and platinum wire acts as the counter electrode. Prior to each experiment, the working electrode was dipped in HCl solution without and with different concentrations of the extract for 30 min to reach the steady-state open circuit potential (OCP). After that, electrochemical impedance spectroscopy (EIS) experiment was performed by applying a frequency range from 100 kHz to 0.01 Hz at an AC voltage amplitude of 10 mV. Nyquist and Bode plots were used to represent the EIS data, and Zview software was used to obtain the appropriate equivalent circuit model. All tests were performed in an aerated and non-stirred condition. Then, the potentiodynamic polarization experiment was achieved in the potential range of -800 to -200 mV/SCE applying a sweep rate of 0.5 mV/s. The corrosion current density (i_{corr}), anodic Tafel slope (β_a), cathodic Tafel slope (β_c), and corrosion potential (E_{corr}) were determined using Nova 2.1 program. The following relationship was used to quantify inhibition efficiency ($\eta_{PPC}\%$) using the calculated values of i_{corr} .

$$\eta_{PPC}(\%) = \frac{i_{corr}^{(0)} - i_{corr}^{(i)}}{i_{corr}^{(0)}} \times 100 \quad (3)$$

where $i_{corr}^{(0)}$ and $i_{corr}^{(i)}$ symbolize the corrosion current densities of blank reference and inhibited medium, respectively.

Applying polarization resistance (R_p) obtained from the impedance data of the Nyquist plots, the $\eta_{EIS}\%$ was measured.

$$\eta_{EIS}(\%) = \frac{R_p^{(i)} - R_p^{(0)}}{R_p^{(i)}} \times 100 \quad (4)$$

where $R_p^{(0)}$ and $R_p^{(i)}$ symbolize the polarization resistances of blank reference and inhibited medium, respectively.

2.3.4. SEM analysis

A scanning electron microscope (SEM) was used for surface characterization of the carbon steel. Steel samples were treated as described above before immersion in inhibited solution for 12 h before tests. A Hitachi TM-1000 SEM at an accelerating voltage of 15 kV was used for SEM analysis of steel surface.

2.4. Theoretical calculations

The geometry optimization and frontier molecular orbitals of the main components of AVU extract were determined using the Dmol3 module implemented in Material Studio software [27] using Generalized gradient approximation (GGA) with double numerical basis sets plus polarization (DNP) [28] and

COSMO solvation model [29]. All other parameters correspond to “fine” quality in the Dmol3 code.

MD simulation by Forcite module of Materials Studio software was used to investigate the interaction of the four main components of AVU extract with Fe(110) surface. The pure iron crystal was imported from Materials Studio database and cleaved along (110) plane. Then, the Fe (110) plane of four layers was enlarged to 6×6 supercell, and a vacuum slab with a zero thickness was created. Fe (110) plane was chosen as the first layer as it is the most stable iron plan. The second layer that contains one AVU extract’s components, 491 water molecules, $9\text{H}_3\text{O}^+$ and 9Cl^- was created by Amorphous cell module of Materials Studio. Then, both layers were combined by Build layers tool of Materials Studio, and the resulted simulation box had a dimension of $12.39 \times 12.39 \times 35.97 \text{ \AA}^3$. Although the simulation system is a simplistic model of the corrosion inhibition process, it is still useful in making qualitative and comparative analyses, which can boost the understanding of the inhibitor’s adsorption behavior. Other parameters were COMPASS force field, NVT ensemble, 303 K, 5000 ps simulation time, and 1 fs time step. The energy of interaction between molecules and Fe(110) surface was determined according to the following equation:

$$E_{interaction} = E_{total} - (E_{surface+solution} + E_{inhibitor}) \quad (5)$$

where E_{total} , $E_{surface+solution}$, $E_{inhibitor}$ are the system’s energies, the Fe surface and solvent layer, and the inhibitor molecule alone, respectively.

3. Results and discussion

3.1. Identification of AVU extract’s components

Fourty six chemicals accounting for 89.89% of the overall chemical composition of *Ammi visnaga* umbels’ methanolic extract were found (Table 1). The Edulisin III is the most abundant component, accounting for 72.88% of the total composition, followed by Binapacryl (4.32%), then Khellin (1.97%), and Visnagin (1.65%) with modest percentages.

The molecular structures and organic class of major constituents of the methanolic extract of *Ammi visnaga* umbels are listed in Table 2. According to data from the literature, GC-MS analysis of the methanolic extract of *Ammi visnaga* umbels has not been studied to date; however, the two main furanochromones (khellin and visagin) have already been isolated in several studies (Franchi et al., 1985) using different methods such as the capillary electrophoresis method (Günaydin and Erim, 2002). Moreover, with a new supercritical fluid extraction technique, these active principles were studied and then analyzed by reverse-phase HPLC [41] and separated in different stages of development of the fruit of *Ammi visnaga* (Bishr et al., 2018). In contrast, binapacryl and Edulisin III were never identified in extracts of *Ammi visnaga*. However, Edulisin III was previously isolated in (Mizuno et al., 1994) from the fruit of *Angelica edulis* Miyabe (Umbelliferous).

3.2. Gravimetric measurements

3.2.1. Effect of AVU extract concentration

The gravimetric experiment was carried out to determine AVU extract’s protective capability at successively increasing

Table 1 Chemical Composition of the Raw Methanolic Extract of *Ammi Visnaga umbels* identified by GC–MS.

| N ^o | Compound | Retention time | % |
|----------------|--|----------------|---------------|
| 1 | Dimethylethylamine | 5.478 | 0.623 |
| 2 | 4-Ethyl-2,3-dihydrofuran | 5.823 | 0.034 |
| 3 | 3-Oxobutyramide | 7.597 | 0.434 |
| 4 | Linalol | 24.346 | 0.176 |
| 5 | <i>cis</i> -3-Hexenyl <i>iso</i> -butyrate | 30.962 | 0.310 |
| 6 | 2,6-Dimethyl-1,7-octadiene-3,6-diol | 36.554 | 0.175 |
| 7 | (Z)-2-nonadecene | 44.287 | 0.069 |
| 8 | Neryl (S)-2-methylbutanoate | 50.973 | 0.043 |
| 9 | 2,4-Bis-(tert.-butyl)-phenol | 51.187 | 0.070 |
| 10 | Geranyl vinyl ether | 61.777 | 0.055 |
| 11 | Dodecyl isobutyrate | 64.374 | 0.180 |
| 12 | Estragole | 65.080 | 0.063 |
| 13 | Farnesol | 67.237 | 0.761 |
| 14 | Visnagin | 77.561 | 1.658 |
| 15 | 2-(2-vinylcyclohexyl)-3-butyn-2-ol | 79.329 | 0.194 |
| 16 | <i>cis</i> , <i>trans</i> -.alpha.-Farnesene | 84.694 | 1.127 |
| 17 | Khellin | 86.049 | 1.977 |
| 18 | Isopimpinellin | 86.164 | 0.199 |
| 19 | Butyl 4,7,10,13,16,19-docosahexaenoate | 86.239 | 0.125 |
| 20 | Doconexent | 87.821 | 0.746 |
| 21 | Caryophyllene oxide | 89.076 | 0.133 |
| 22 | Glyceryl linolenate | 92.251 | 0.076 |
| 23 | 5.alpha.-Estran-3-on-17.beta.-ol | 92.306 | 0.042 |
| 24 | 2-Methylenecholestan-3-ol | 92.965 | 0.083 |
| 25 | Isolongifolene | 96.145 | 0.126 |
| 26 | Decursin | 98.188 | 0.464 |
| 27 | Cnidimine | 100.341 | 1.949 |
| 28 | Edulisin III | 104.128 | 72.886 |
| 29 | Binapacryl | 107.090 | 4.325 |
| 30 | Docosane | 112.464 | 0.379 |
| 31 | Andrographolide | 121.942 | 0.409 |
| | Total | | 89.891 |

concentrations. Table 3 lists the derived parameters such as corrosion rate ($\text{mg cm}^{-2}\text{h}^{-1}$), surface coverage, and inhibition efficiency (percentage). According to the findings, AVU extract may effectively resist carbon steel corrosion under tested acidic medium. Furthermore, when the concentration of the inhibitor increases, the corrosion rate reduces, thus the corrosion-preventive activity of AVU extract improves with concentration, with the greatest concentration being 700 ppm. The ability of AVU extract's natural chemical constituents to adsorb onto the metal surface is mainly the reason for its corrosion resistance ability. The synergistic adsorption of different AVU extract's components may create a protective barrier on the steel surface, thus protecting it against the extrinsic attack of acidic solution's aggressive ions (Aslam et al., 2020). The proportion of surface covered with adsorbed AVU extract molecules determines the amount of corrosion protection. The adsorbed molecules of AVU extract grow on the metal surface as its concentration increases. The θ value, is a critical variable since it reflects the percentage of metal substrate surface covered by AVU extract molecules.

3.2.2. Effect of temperature and activation parameters

Considering the well-known effect of temperature on most of chemical reactions, a better understanding of the corrosion

inhibition process can be achieved by studying the effect of temperature on the inhibition performance of tested inhibitor. To this end, the effect of temperature on the corrosion rate is investigated using weight loss experiments at four different temperatures in the range of 303–333 K with 10 K gap. Results are represented in Table 4. It can be seen that the increase of temperature accelerates the metal dissolution rate in both uninhibited and inhibited mediums. However, the addition of the optimum concentration of AVU extract to the 1.0 mol/L HCl results in a significant decrease of corrosion rate compared to uninhibited solutions. The maximum inhibition efficiency is obtained at 303 K; however, it shows only a small decrease by 5% at 333 K, signifying that the presence of AVU extract in the blank solution has an excellent corrosion inhibition effect.

The reaction kinetics of corrosion follow Arrhenius and transition state equations as follow:

$$C_R = k \exp\left(\frac{-E_a}{RT}\right) \quad (6)$$

$$C_R = \frac{RT}{Nh} \exp\left(\frac{\Delta S_a}{R}\right) \exp\left(\frac{-\Delta H_a}{RT}\right) \quad (7)$$

where A is the Arrhenius pre-exponential factor, E_a is the activation energy, T is the absolute temperature, N is Avogadro's number, R is the gas constant, h is Plank's constant.

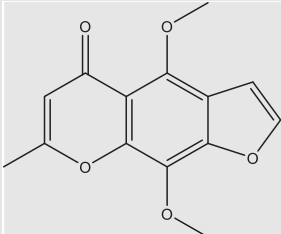
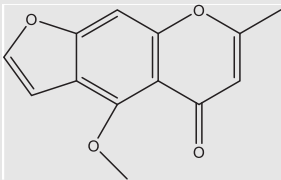
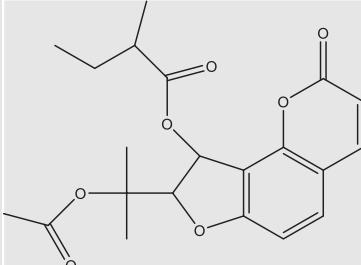
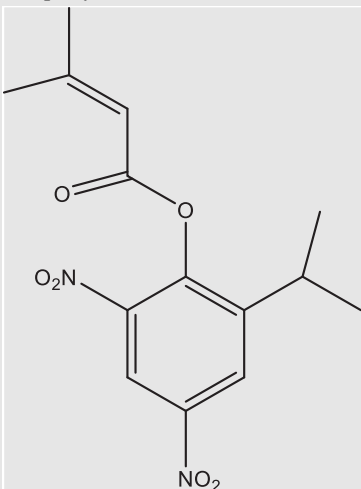
Plots of $\ln C_R$ vs. $1000/T$ and $\ln C_R/T$ vs. $1000/T$ are shown in Fig. 1(a) and 1(b), representing Arrhenius and transition state equations, respectively. Activation parameters calculated from slopes and intercept of plots are listed in Table 5. Results show a higher activation energy in the presence of AVU extract compared to that of blank solution. It suggests the increase of the energy barrier for the corrosion reaction, resulting in reduced rate of corrosion process (Verma et al., 2016). The positive ΔH_a values refer to the endothermic nature of the dissolution process (Azzaoui et al., 2017). Besides, the increased ΔS_a value signifies an increase in the degree of disorder compared with the blank (Azzaoui et al., 2017).

3.3. Electrochemical impedance spectroscopy

The EIS is a non-destructive and very effective instrumental approach for determining the corrosion processes occurring at the metal-corrosive electrolyte interface. Fig. 2(a) shows Nyquist curves for carbon steel in a 1.0 mol/L HCl solution with and without different AVU extract concentrations. The diameter of capacitive loops is directly related to inhibitor concentration, implying that greater concentrations of AVU extract might more effectively protect against the attack of aggressive acidic species. The single semicircle can be ascribed to the charge transfer process at the solution/electrode interface (Aslam et al., 2019). The charge transfer process controls the corrosion reaction of steel, and the inhibitor presence does not change the steel dissolution mechanism (Znini et al., 2012). It is also clear that these semicircles are imperfect due to the frequency dispersion (Larabi et al., 2004).

The circuit $R_s(R_p\text{CPE})$ shown in Fig. 2(b) is used to model the impedance output explicitly. R_s , R_p , and CPE represent solution resistance, polarization resistance, and the constant phase element, respectively. To address the fluctuations in capacitance behavior, CPE is employed instead of capacitance

Table 2 Molecular structures and organic class of the major constituents of the methanolic extract of *Ammi visnaga* umbels.

| Compounds | Chemical group | Chemical formula | (%) |
|---|----------------|----------------------|-------|
| Khellin  | Furanochromons | $C_{14}H_{12}O_5$ | 1.97 |
| Visnagin  | | $C_{13}H_{10}O_4$ | 1.65 |
| Edulisin III  | Coumarins | $C_{21}H_{24}O_7$ | 72.88 |
| Binapacryl  | Dinitrophenols | $C_{15}H_{18}N_2O_6$ | 4.32 |

(Bahlakeh et al., 2019b; Dehghani et al., 2020a). The following relationship may be used to calculate the CPE impedance (Z_{CPE}) (Orazem and Tribollet, 2008).

$$Z_{CPE} = Y_0^{-1}(j\omega)^{-n} \quad (8)$$

here, Y_0 represents proportionality constant, n is the CPE exponent, which ranges from -1 to $+1$ and j is an imaginary number ($j = (-1)^{1/2}$). ω is the angular frequency in rad^{-1} . C_{dl} is estimated by the following equation (Saha et al., 2016a):

$$C_{dl} = Y_0(\omega_{max})^{(n-1)} \quad (9)$$

where, ω_{max} is the frequency at which impedance is maximum.

C_{dl} may also be represented as follows:

$$C_{dl} = \frac{\epsilon\epsilon_0}{d} S \quad (10)$$

where d is the thickness of the double layer, ϵ_0 is the permittivity of free space, ϵ is the local dielectric constant, and S is the surface area of the electrode.

Table 3 Corrosion parameters obtained from weight loss measurements of carbon steel in 1.0 mol/L HCl at various concentrations of AVU extract at 303 K.

| [AVU] (ppm) | C_R (mg cm ⁻² h ⁻¹) | θ | η_w (%) |
|-------------|--|----------|--------------|
| 1.0 M HCl | 1.135 ± 0.0072 | – | – |
| 150 | 0.5108 ± 0.0098 | 0.55 | 55 |
| 250 | 0.3746 ± 0.0076 | 0.67 | 67 |
| 450 | 0.2384 ± 0.0047 | 0.79 | 79 |
| 700 | 0.1817 ± 0.0088 | 0.84 | 84 |

Table 6 shows the electrochemical parameters acquired from the EIS results using the equivalent circuit. It can be shown in Table 6 that when AVU extract is present in the acid solution, R_p values increase, and C_{dl} values decrease in contrast to the untreated media. Furthermore, as the AVU extract concentration is raised between 150 and 700 ppm, the R_p values rise. In contrast, the C_{dl} values fall, indicating a significant double-layer behavior change due to AVU extract adsorption onto the steel substrate. It can be explained by an increased thickness and/or decreased local dielectric constant, as Helmholtz model suggested (Fouda et al., 2013). This adsorption occurred simultaneously with the displacement of H₂O molecules or other ions from the steel substrate. As a consequence of the successful adsorption of AVU extract molecules on the steel surface, a drop in the rate of corrosion and an increase in inhibitory efficiency are observed.

The impedance response of AVU extract's addition to HCl solution can also be obtained in Bode modulus and Bode phase graphs, as illustrated in Fig. 2(c). Compared to the corrosive electrolytic solution, the phase angle increases to greater values with larger concentrations of AVU extract in the middle frequency domain, implying the formation of a protective barrier that provides a superior capacitance response in the presence of AVU extract. Furthermore, relative to the corrosive electrolyte reference, the magnitudes of absolute impedance in the lower frequency zone have been moved towards greater values. This confirms the Nyquist representation's conclusion, and both show the effective adsorption of AVU extract's molecules onto the steel surface, preventing it, therefore, from corrosion. As shown in Table 2, AVU extract composition contains many molecules with several heteroatoms, aromatic rings, and double bonds. These would work as adsorption sites when AVU extract is added to the acidic solution, interacting with the steel surface via physical and chemical interactions.

These reactive sites will be investigated in more detail in the theoretical sections.

3.4. Effect of different immersion times

The effect of immersion time on the protective layer developed on the surface can be determined by observing the evolution of the polarization resistance of carbon steel at various immersion times in an aggressive environment without and with the inclusion of the inhibitor. Carbon steel samples were subjected for 0.5–24 h to the solutions containing a higher concentration of AVU extract, i.e., 700 ppm. Fig. 2(d) illustrates the recorded electrochemical impedance diagrams in the form of Nyquist plots. Table 7 shows the electrochemical parameter values obtained using the equivalent circuit model after curve processing. The results show that on increasing immersion time from 0.5 to 12 hr, the R_p values decrease in the uninhibited and inhibited medium. However, the values of R_p remain significantly higher compared with blank solution. When the immersion time is increased from 12 to 24 hrs., some of the adsorbed AVU extract molecules are mainly desorbed from the carbon steel surface. As a result, the surface area covered decreased. However, since the performance is directly related to the blank solution, it can be noticed that the AVU extract is highly effective when the steel dissolution is very high (24 h, $R_p = 12$ Ohm cm² compared to 63 Ohm cm² in the presence of AVU extract). On the basis of the experimental results, it can be said that the AVU extract can act as an excellent acid corrosion inhibitor under present experimental conditions.

3.5. Potentiodynamic polarization curves

Open circuit potential plots and potentiodynamic polarization curves for carbon steel samples excluding and including varying concentrations of AVU extract in 1.0 mol/L HCl medium are represented in Fig. 3(a)-(b). Derived parameters and inhibition efficiencies ($\eta_{PPC}\%$) are listed in Table 8. From OCP plots (Fig. 3(a)), it can be noticed that a steady state potential is attained in the absence and in the presence of different concentrations of AVU extract. The steady state potential values of carbon steel in the presence of inhibitor's concentrations are all around that of blank solution, without significant potential shifting, suggesting a mixed inhibition effect. A careful analysis of Tafel curves expresses that cathodic as well as anodic arms got altered when AVU extract is added into acidic medium, and the curves moved towards lower corrosion current densities on adding accretive concentrations of AVU extract in

Table 4 Corrosion rate and inhibition efficiency of carbon steel in 1.0 mol/L HCl in the absence and in presence of 700 ppm of AVU extract at different temperatures.

| Medium | 303 K | | 313 K | | 323 K | | 333 K | |
|-----------------------------|--|--------------|--|--------------|--|--------------|--|--------------|
| | C_R (mg cm ⁻² h ⁻¹) | η_w (%) | C_R (mg cm ⁻² h ⁻¹) | η_w (%) | C_R (mg cm ⁻² h ⁻¹) | η_w (%) | C_R (mg cm ⁻² h ⁻¹) | η_w (%) |
| Blank | 1.135 | – | 2.466 | – | 5.032 | – | 10.029 | – |
| Blank + 700 ppm AVU extract | 0.181 | 84 | 0.443 | 82 | 0.956 | 81 | 2.107 | 79 |

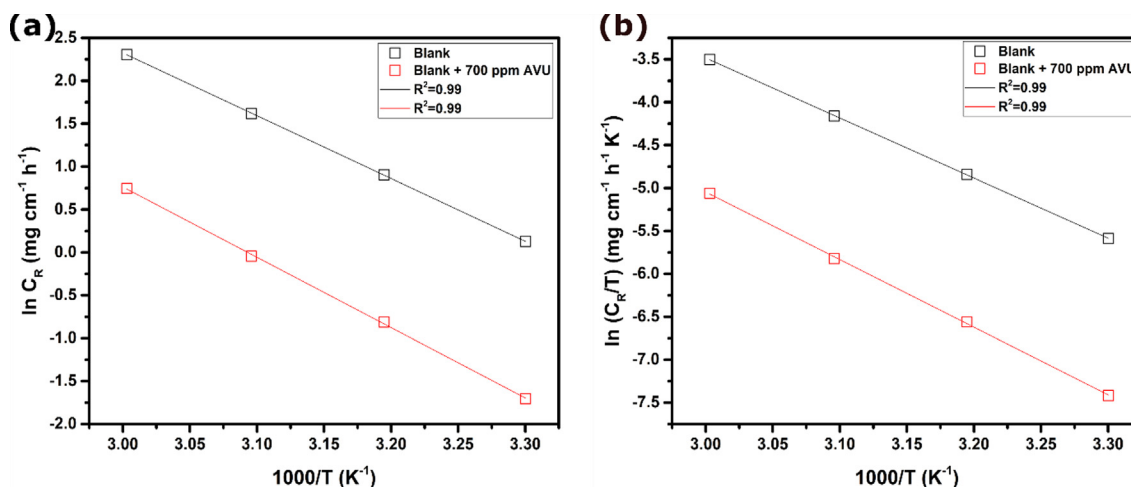


Fig. 1 Arrhenius (a) and transition state (b) plots for carbon steel in 1.0 mol/L HCl without and with 700 ppm of AVU extract.

acidic solution. It affirms that AVU extract limited both steel oxidation and hydrogen ions' reduction at carbon steel surface. As reported in the literature (Palaniappan et al., 2019), a compound can be labeled as anodic/cathodic type when the shift in E_{corr} is at least 85 mV with respect to blank solution. By inspecting the data in Table 8, it can be detected that the AVU extract in the considered system functioned as a mixed-type inhibitor. These results substantiated that the investigated AVU extract significantly lowered the anodic dissolution reaction and moderately cathodic reaction to some extent. The values of the cathodic slopes β_c vary delicately with the addition of the green inhibitor, unlike the anode slopes β_a , which fluctuate a little more, which declares the methanolic extract of the umbels as a mixed inhibitor.

3.6. Surface characterization by SEM

SEM is a reliable tool to analyze the surface and morphologies of a wide range of materials. SEM can monitor the surface change during corrosion inhibition. The morphology of the carbon steel surface in the absence and in the presence of 700 ppm g/L of AVU extract in 1.0 mol/L HCl solution is represented in Fig. 4. By inspecting this Figure, differences can be easily distinguished between protected and unprotected steel surface. The unprotected surface (Fig. 4(a)) is seriously corroded, and there is the formation of corrosion products. According to our recent XPS analysis, those corrosion products are mainly iron oxides such as FeO/Fe₃O₄, and Fe₂O₃ due to the iron oxidation and chloride attack (Lgaz et al., 2020b). In contrast, no severe corrosion attack is observed on the steel surface after adding 700 ppm of AVU extract to HCl solution. It signifies that the AVU extract can inhibit the acid solution and limit its aggressiveness during the immersion. As evidenced by previous results, this can be explained by the effective adsorption of different AVU extract's components, forming a robust protective barrier against corrosion.

3.7. DFT calculations

Quantum chemical calculations are recognized as one of the most efficient tools to get information about the electronic

and reactivity of chemical compounds (Boulhaoua et al., 2021; Guo et al., 2020). These calculations find broad applications in corrosion inhibition studies (Bahlakeh et al., 2019a; Olanokanmi et al., 2020). Global reactivity descriptors like Highest Occupied Molecular Orbitals (HOMO), Lowest Unoccupied Molecular Orbitals (LUMO), and energy gap (ΔE_{gap}), etc. can be obtained from DFT calculations. These parameters are related to a single molecule; therefore, they have two advantages and one limitation. They allow the identification of potential adsorption sites and reactivity of the investigated molecule, and further the comparison of this reactivity with other molecules, which gives initial insights on why a molecule is more reactive than others (Fan et al., 2019; Liu et al., 2021b, 2021a). However, the main limitation of this approach is that it focusses only on the single molecule without considering its interaction with the surface of the metal (Kumar et al., 2020; Poberžnik et al., 2020). In this work, the AVU extract is regarded as one inhibitor even though it contains many components. Therefore, efforts will be limited to investigating frontier molecular orbitals *iso*-surfaces of the four molecules with higher percentages and the local reactivity of the Edulisin III, which is believed to be the main responsible for the corrosion inhibition effect of the AVU extract. Fig. 5 represents the *iso*-surfaces of the HOMO and LUMO of Edulisin III, Bina-pacryl, Khellin, and Visnagin. The HOMO density is related to the ability of a molecule or a part of it to donate electrons (Dutta et al., 2017; Meng et al., 2021). The inspection of results in Fig. 5 reveals that the HOMO density is distributed over the chromone moiety of the Edulisin III, suggesting that this part may be responsible for donating electrons to vacant *d*-orbitals of iron upon its adsorption.

Table 5 The activation parameters for carbon steel in 1.0 mol/L HCl with and without addition of 700 ppm of AVU extract.

| Medium | E_a (kJ/mol) | ΔH_s^o (kJ/mol) | ΔS_a^o (J/mol K) |
|-------------|----------------|-------------------------|--------------------------|
| Blank | 60.79 | 58.15 | -51.86 |
| AVU extract | 68.09 | 65.46 | -42.92 |

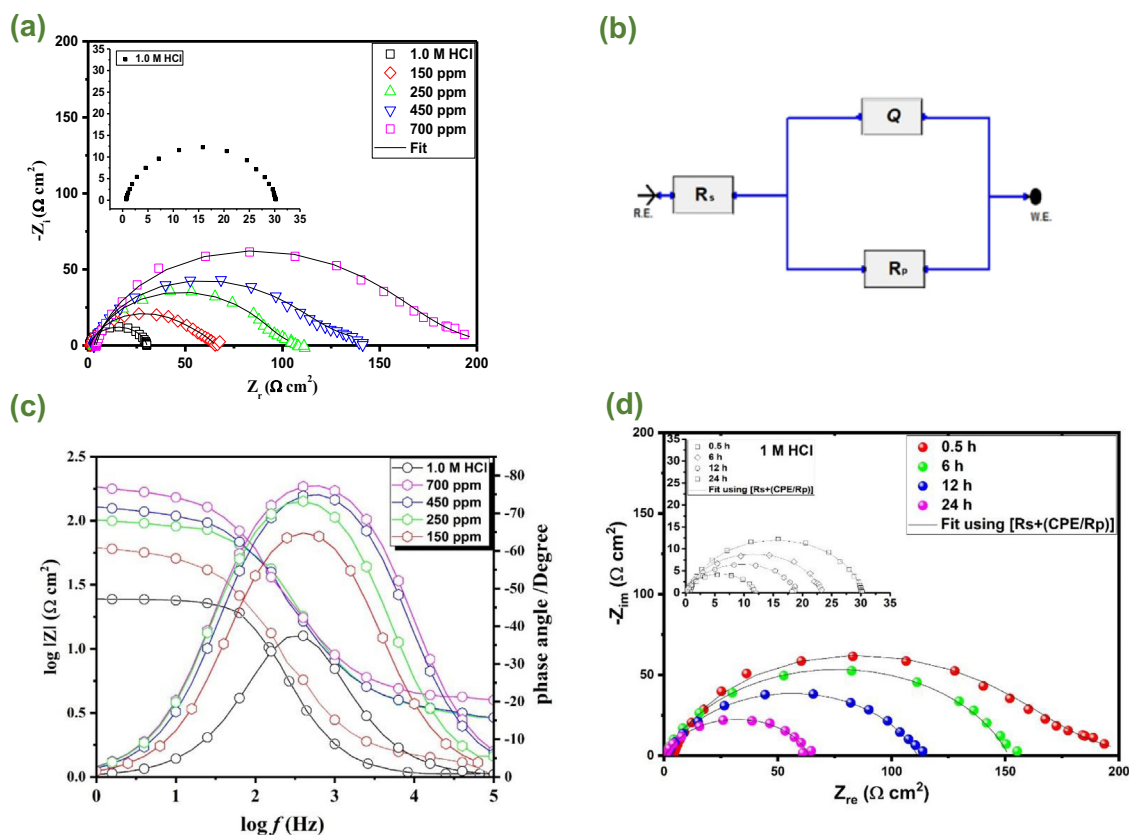


Fig. 2 Impedance results of carbon steel in 1.0 mol/L HCl without and with different concentrations of AVU extract at 303 K; (a) Nyquist plots, (b) Equivalent electrical circuit, (c) Bode plots, and (d) Nyquist plots of carbon steel in 1.0 mol/L HCl and with 700 ppm of AVU extract at different immersion times.

In the other three molecules, i.e., Binapacryl, Khellin, and Visnagin, the HOMO density is observed on the entire molecular structure. It signifies that the whole molecule can be involved in interactions with the steel surface. Moving to the LUMO *iso*-surfaces, which indicate the tendency of a molecule to accept electrons from the metal surface. This is usually described as a back-donation process (Saha et al., 2016b). In the case of Edulisin III, the LUMO distribution is like that of HOMO, i.e., over the chromone moiety, suggesting that it is the main reactive part and responsible for Donor-Acceptor (D-A) interactions with iron atoms. Interestingly, the same goes for other molecules with intensities a bit lower than HOMO *iso*-surfaces. These remarks can be explained by the

presence of several heteroatoms, especially the oxygen atom and aromatic rings. The oxygen atom can donate its electron pairs when interacting with vacant *d*-orbitals of iron. On the other hand, the back-donation of electrons to π^* orbitals is an important step in strengthening bonds and coordination with the metal surface.

Condensed Fukui functions *iso*-surfaces of the Edulisin III molecule are shown in Fig. 6. A large *iso*-surface represents a high Fukui function value and indicates that the atom or part of the molecule is chemically softer than other parts (Damej et al., 2021; El Aoufir et al., 2020). Fig. 6(a) shows parts of Edulisin III susceptible to be attacked by nucleophiles, while Fig. 6(b) shows those atoms or parts susceptible to be attacked

Table 6 Impedance parameters for corrosion of carbon steel in 1.0 mol/L HCl in the absence and presence of different concentrations of AVU extract at 303 K.

| [AVU extract] (ppm) | R_p ($\Omega \text{ cm}^2$) | n | $Y_0 \cdot 10^{-4}$ ($\text{s}^n \Omega^{-1} \text{ cm}^{-2}$) | C_{dl} ($\mu\text{F cm}^{-2}$) | $\chi^2 \times 10^{-3}$ | η_{EIS} (%) |
|---------------------|---------------------------------|------|--|------------------------------------|-------------------------|-------------------------|
| 1.0 mol/L HCl | 29.35 | 0.89 | 1.7610 | 92 | 0.33 | – |
| 150 | 68.46 | 0.86 | 1.6601 | 80.09 | 6.08 | 57 |
| 250 | 97.84 | 0.84 | 1.4612 | 65.06 | 3.87 | 70 |
| 450 | 122.89 | 0.84 | 1.1632 | 51.79 | 4.65 | 74 |
| 700 | 172.66 | 0.85 | 0.7870 | 36.86 | 5.23 | 83 |

Table 7 Electrochemical impedance and inhibition efficiency parameters for carbon steel samples in 1.0 mol/L HCl without and with 700 ppm of AVU extract at various times.

| Inhibitor and Time (h) | $R_p/\Omega\text{cm}^2$ | n | $Q \times 10^{-4}/S^n \Omega^{-1} \text{cm}^{-2}$ | $C_d/\mu\text{F cm}^{-2}$ | $\chi^2 \times 10^{-3}$ | $\eta_{EIS}/\%$ |
|------------------------|-------------------------|------|---|---------------------------|-------------------------|-----------------|
| Blank | | | | | | |
| 0.5 | 29 | 0.89 | 1.7610 | 92 | 0.33 | – |
| 6 | 23 | 0.84 | 2.5114 | 94 | 2.45 | – |
| 12 | 18 | 0.83 | 2.9866 | 102 | 3.24 | – |
| 24 | 12 | 0.88 | 3.0891 | 144 | 1.14 | – |
| AVU extract | | | | | | |
| 0.5 | 172 | 0.85 | 0.7870 | 36 | 5.23 | 83 |
| 6 | 150 | 0.85 | 0.8181 | 37 | 7.36 | 84 |
| 12 | 110 | 0.83 | 1.0032 | 39 | 5.47 | 83 |
| 24 | 63 | 0.86 | 1.0527 | 46 | 3.27 | 81 |

by electrophiles. Results in Fig. 6 strengthen the conclusion that the chromone moiety is the most reactive part in the Edulisin III molecule. It is responsible for almost all D-A interactions of these components with steel surface, thus making a vital contribution to the corrosion inhibition performance of the investigated extract.

3.8. Molecular dynamics simulation

The corrosion inhibition of carbon steel by organic molecules is an adsorption process. The reactive sites of the molecules interact with the steel surface through physical and or chemical interactions. Therefore, a reliable simulation of the corrosion inhibition should involve both interactive species, i.e., molecule and the metal. To this end, researchers have turned their attention towards molecular dynamics simulation for getting useful insights into the adsorption process (Verma et al., 2018b). In this work, MD simulation was performed for the four main components of AVU extract. Fig. 7 shows the top and side views of the most stable adsorption geometries. The adsorption systems include one molecular structure of the components along with water molecules, chlorine, and hydronium ions in interaction with Fe(110) surface. It can be seen that after the simulation equilibrium, all components tend to move close to the iron surface.

Interestingly, all aromatic rings adopt a parallel configuration over the Fe(110). This remark strengthens the DFT results, which showed that aromatic rings are highly reactive parts. The parallel adsorption mode gives a chance to strong D-A interactions and thus high coverage of the surface. The calculated interaction energies of the Edulisin III, Binapacryl, Khellin, and Visnagin over Fe(110) surface are -324.5 , -241.7 , -306.5 , and -297.4 kJ/mol, respectively. It indicates that all components strongly interact with Fe(110) surface, with Edulisin outperforms other molecules.

3.9. Comparison with similar materials

Recently, there has been a great effort towards developing green and eco-friendly alternatives to traditional, especially toxic corrosion inhibitors (Afia et al., 2013; Bammou et al., 2014; Oguzie et al., 2012). Besides, the development of conven-

tional organic inhibitors comes with other unwanted issues related to expensive solvents, reagents, and catalysts and environmental problems due to the discharge of chemicals into the surrounding environments. These factors and others have turned the researchers' attention to more safe alternatives such

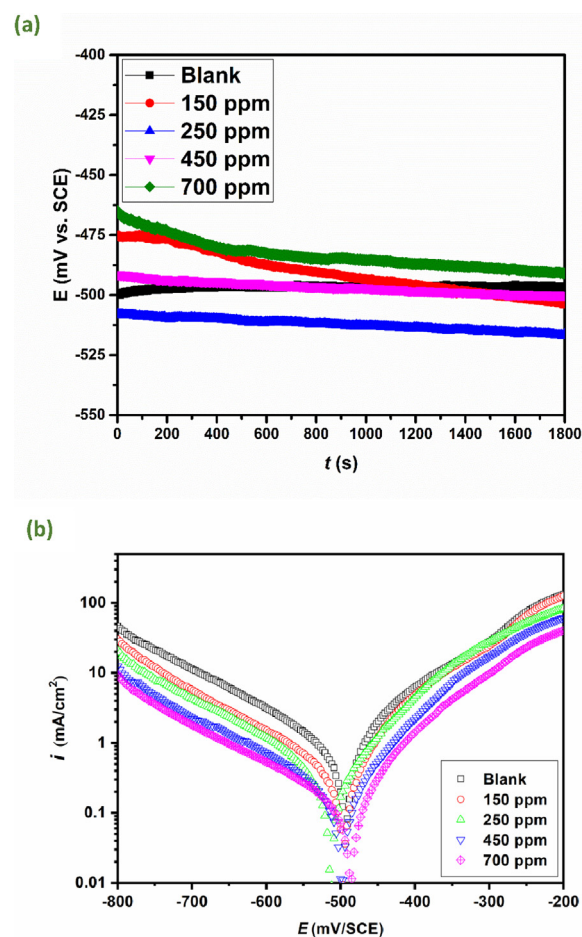
**Fig. 3** Open circuit potential plots (a) and polarization curves (b) of carbon steel in 1 mol/L HCl with and without addition of different concentrations of AVU extract at 303 K.

Table 8 Electrochemical parameters and corrosion inhibitory efficacy of steel in 1.0 mol/L HCl without and with the addition of 303 K of AVU extract.

| [AVU extract] (ppm) | $-E_{\text{corr}}$ (mV/SCE) | $-\beta_c$ (mV dec $^{-1}$) | β_a (mV dec $^{-1}$) | i_{corr} ($\mu\text{A cm}^{-2}$) | η_{Tafel} (%) |
|---------------------|-----------------------------|------------------------------|-----------------------------|---|---------------------------|
| 1.0 M HCl | 496.0 | 87.5 | 139.7 | 576.0 | – |
| 150 | 503.2 | 78.5 | 132.6 | 276.36 | 55 |
| 250 | 517.7 | 76.1 | 137.1 | 180.48 | 67 |
| 450 | 500.4 | 71.7 | 133.1 | 129.72 | 79 |
| 700 | 491.3 | 76.3 | 147.1 | 107.16 | 84 |

as plant-based materials. Since then, many new environmentally friendly corrosion inhibitors have appeared and applied for protecting different metals and alloys. In the literature, several review papers report the application of plant-based materials in different experimental conditions (Alrefaee et al., 2021), and references therein. Herein, for a comparative purpose, a few plant-based corrosion inhibitors are listed in Table 9 with some experimental conditions. All reported inhibitors have been investigated in experimental conditions similar to the present work. Generally speaking, a plant-based corrosion inhibitor with an inhibition efficiency over 80% in a highly acidic solution has a great industrial application potential given its non-toxic nature and, therefore, the possibility for application in low corrosive mediums. However, reported results show that most inhibitors have high corrosion inhibition performance. The extract under investigation shows an inhibition efficiency of 84% at a very low concentration of 700 ppm. Compared with some reported results, and considering concentration/efficiency relationship, the present extract has excellent corrosion inhibiting properties, which outperforms most reported ones. Together, these promising results once again demonstrates the importance of this class of materials for protecting metals in highly aggressive solutions.

3.10. Corrosion inhibition mechanism

Experimental results showed that the addition of tested inhibitor to the 1.0 mol/L HCl solution decreased the double layer

capacitance compared to that obtained in the blank solution. Moreover, a substantial decrease is observed in both anodic and cathodic corrosion reactions after the addition of AVU extract to 1.0 mol/L solution. These conclusions suggest that AVU extract's components act mainly by adsorption on the steel surface, increasing the double layer thickness, and therefore decreasing its capacitance. Unsurprisingly, most organic corrosion inhibitors have similar inhibition mechanism; that is the adsorption on steel surface by replacing pre-adsorbed water molecules (Fan et al., 2021; Ma et al., 2020). This adsorption is usually a two-step process.

- The steel surface is found to have a positive charge under the same experimental conditions, i.e., 1.0 mol/L (Solmaz, 2014a). Similarly, inhibitor molecules having heteroatoms will be protonated in this acidic medium (Solmaz, 2014b). In this situation, the adsorption of molecules seems impossible due to electrostatic repulsions. However, chlorine ions, which are first pre-adsorb on the positively charged surface, make it possible by playing an intermediate role between protonated molecules and positively charged steel surface (Fan et al., 2020). This process is called physisorption, and it is paramount for the next step.
- The electrostatic attraction between protonated molecules and pre-adsorbed chlorine ions would facilitate the chemical adsorption of AVU extract's components. After approaching the steel surface, molecules having reactive adsorption sites like heteroatoms and π -electrons would

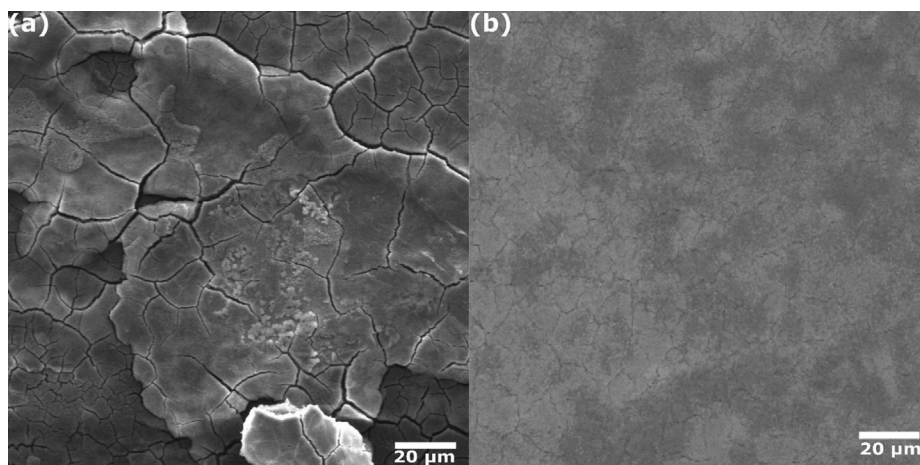


Fig. 4 SEM images of carbon steel in (a) 1.0 mol/L HCl and (b) in presence of 700 ppm of AVU extract after 12 h immersion.

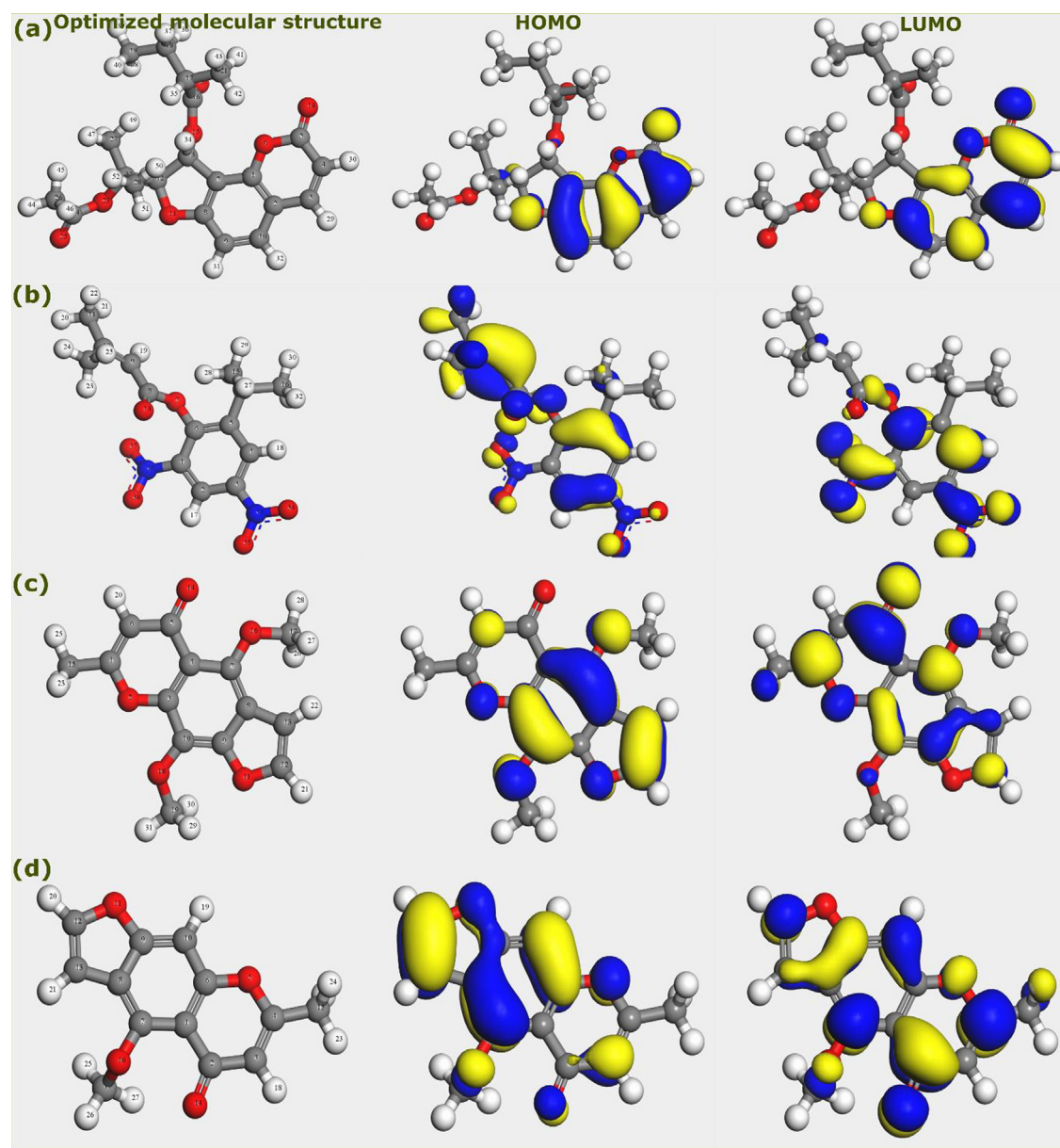


Fig. 5 Optimized molecular structures, HOMO and LUMO *iso*-surfaces of AVU extract's components; (a) Edulisin III, (b) Binapacryl, (c) Khellin, and (d) Visnagin.

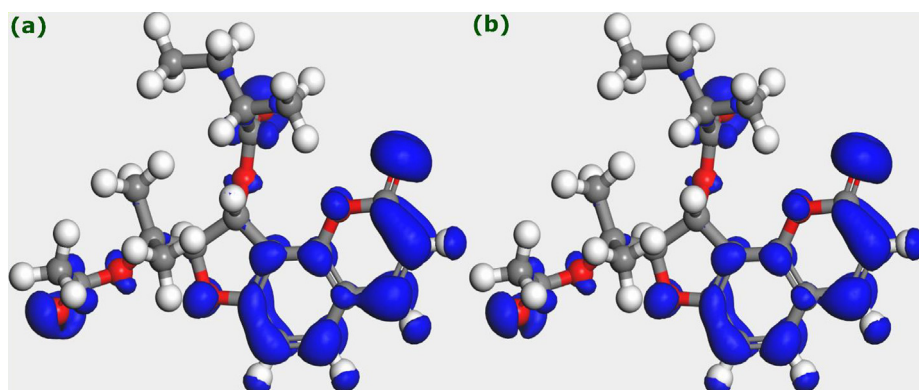


Fig. 6 Fukui function *iso*-surfaces of Edulisin III, (a) f^+ , and (b) f^- .

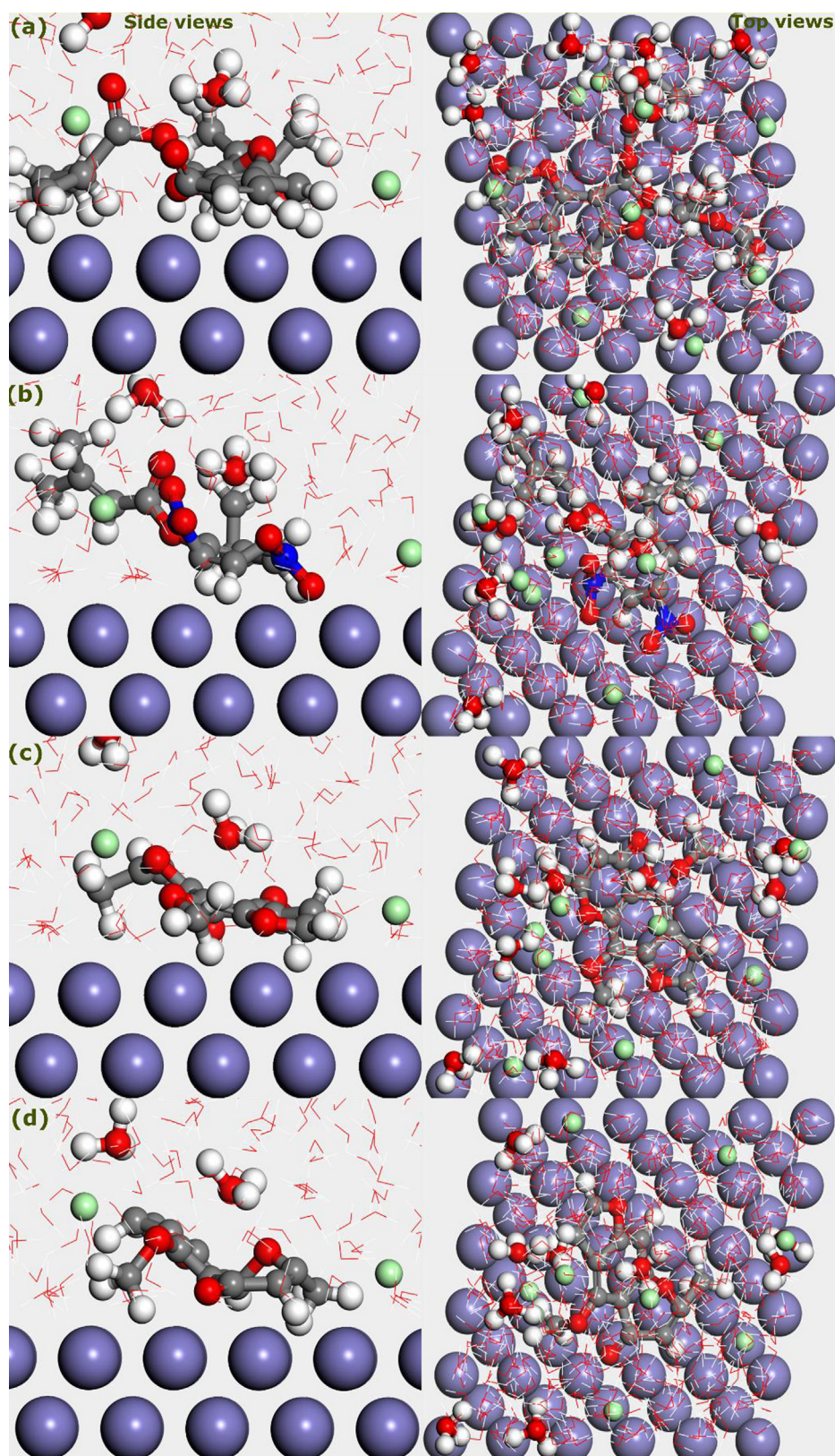


Fig. 7 Top and side views of the most stable geometries of AVU extract's components; (a) Edulisin III, (b) Binapacryl, (c) Khellin, and (d) Visnagin.

Table 9 The performance and experimental conditions of some previously reported natural-based corrosion inhibitors and AVU inhibitor.

| Inhibitor | Optimum conc./ Material/ Solution | Highest inhibition efficiency (%) | Reference |
|---|-----------------------------------|-----------------------------------|--------------------------------|
| Tunbergia fragrans | 500 ppm/ Mild steel/ 1.0 M HCl | 81.0 | (Muthukumarasamy et al., 2020) |
| Magnolia grandiflora | 500 ppm/ Q235 steel/ 1.0 M HCl | 85.0 | (Chen et al., 2020) |
| Pterocarpus santalinoides leaves extract | 0.7 g/L/ Carbon steel/ 1.0 M HCl | 85.2 | (Dehghani et al., 2020b) |
| Opuntia elatior fruit | 500 mg/L/ Mild steel/ 1.0 M HCl | 79.7 | (Loganayagi et al., 2014) |
| Rosa canina fruit extract | 800 ppm/ Mild steel/ 1.0 M HCl | 86 | (Sanaei et al., 2019) |
| Taxus baccata extract | 600 ppm/ Mild steel/ 1.0 M HCl | 83 | (Hanini et al., 2019) |
| Haematostaphis barteri Leaves Extract | 40 g/L/ Mild steel/ 1.0 M HCl | 73 | (Ishak et al., 2019) |
| Elaeoselinum thapsioides (BEET) butanolic extract | 900 ppm/ Carbon steel/ 1.0 M HCl | 82 | (Benahmed et al., 2020) |
| AVU | 700 ppm/ Mild steel/ 1.0 M HCl | 84 | This work |

participate in chemical interactions with empty *d*-orbitals of iron (Fan et al., 2020). It can be noticed that molecules with high percentage are all having several oxygen atoms. These atoms will act as adsorption sites and share surplus electrons with vacant *d*-orbitals of iron (Haque et al., 2018). Furthermore, it has been shown from MD simulations that all molecules adopt a nearly parallel disposition over the iron surface. This adsorption mode could facilitate the interactions between π -electrons of aromatic rings and the iron atoms. Together, heteroatoms and π -electrons play a significant role in this step, known as a chemisorption process.

- The adsorption of AVU extract's components on steel surface by sharing electrons with vacant *d*-orbitals of iron can lead to the accumulation of electrons on its surface making it more negative. Consequently, to relieve this extra negative charge, the iron surface can transfer electrons to a vacant π^* (antibonding) orbital of the inhibitor molecule via *retro*-donation (Mobin and Rizvi, 2017). This would strengthen the adsorption of molecules and thus leading to an enhanced corrosion protection.

The corrosion inhibition by AVU extract may involve all its components; however, Edulisin III seems to have a higher con-

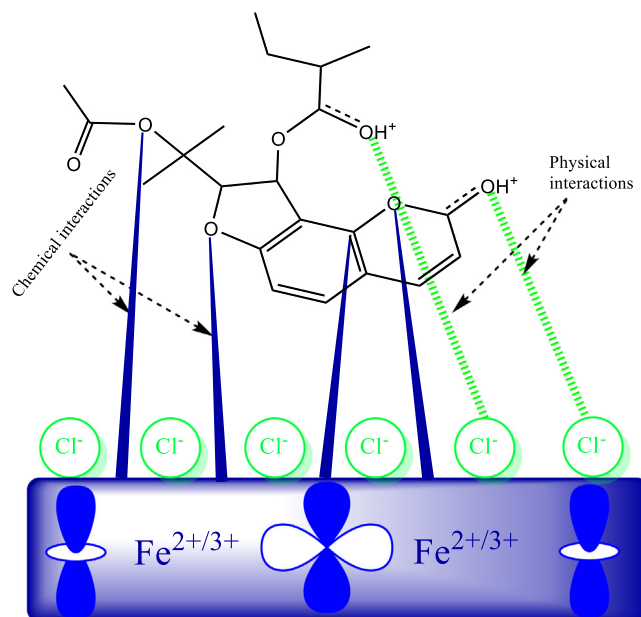


Fig. 8 A graphical representation of the potential corrosion inhibition mechanism; case of Edulisin III.

tribution due to its incomparable percentage with other components. Given this fact, a proposed adsorption mechanism is represented in Fig. 8 taking the Edulisin III as a representative example.

4. Conclusion

In the present work, the corrosion inhibition performance of *Ammi visnaga* extract was investigated for carbon steel in 1.0 mol/L medium employing chemical, electrochemical, surface characterization techniques along with DFT and MD simulation. The characterization of AVU extract by GC/MS revealed the presence of Edulisin III (72.88%), Binapacryl (4.32%), Khellin (1.97%), and Visnagin (1.65%) as major constituents. The AVU's methanolic extract was shown to be a potent corrosion inhibitor for carbon steel in 1.0 mol/L HCl medium, with an inhibition efficacy of 84% at 700 ppm. The extract was found to have a mixed inhibition effect, blocking both anodic and cathodic corrosion reactions. Further, the addition of AVU extract to HCl solution led to a high polarization resistance and a small double-layer capacitance, as evidenced from EIS tests. DFT calculations showed that the chromone moiety of the Edulisin III is the most reactive part, acting simultaneously as electron donating and accepting region. Results from MD revealed that the four components adopted a nearly parallel configuration over the Fe(110) surface. Insights from the present work further highlight the significant advantage of natural-based corrosion inhibitors in protecting metals and alloys.

Declaration of Competing Interest

The authors declare that they have no known competing financial interests or personal relationships that could have appeared to influence the work reported in this paper.

Acknowledgments

The authors would like to thank the Deanship of Scientific Research at Umm Al-Qura University, Saudi Arabia, for supporting this work by Grant Code. 20-SCI-1-01-0002. This research was supported by basic science research program through the National Research Foundation (NRF) of Korea funded by the Ministry of Science, ICT and Future Planning (No. 2015R1A5A1037548).

References

- Abiola, O.K., James, A., 2010. The effects of Aloe vera extract on corrosion and kinetics of corrosion process of zinc in HCl solution. *Corros. Sci.* 52, 661–664.
- Afia, L., Salghi, R., Zarrouk, A., Zarrok, H., Bazzi, E.H., Hammouti, B., Zougagh, M., 2013. Comparative study of corrosion inhibition on mild steel in HCl medium by three green compounds: *Argania spinosa* press cake, kernels and hulls extracts. *Trans. Indian Inst. Met.* 66, 43–49.
- Al-Fakih, A., Aziz, M., Sirat, H., 2015. Turmeric and ginger as green inhibitors of mild steel corrosion in acidic medium. *J. Mater. Environ. Sci.* 6, 1480–1487.
- Alrefaee, S.H., Rhee, K.Y., Verma, C., Quraishi, M.A., Ebenso, E.E., 2021. Challenges and advantages of using plant extract as inhibitors in modern corrosion inhibition systems: Recent advancements. *J. Mol. Liq.* 321, <https://doi.org/10.1016/j.molliq.2020.114666> 114666.
- Aourabi, S., Driouch, M., Kadiri, M., Mahjoubi, F., Sfaira, M., Hammouti, B., Emran, K.M., 2020. Valorization of Zea mays hairs waste extracts for antioxidant and anticorrosive activity of mild steel in 1 M HCl environment. *Arabian J. Chem.* 13, 7183–7198. <https://doi.org/10.1016/j.arabj.2020.08.001>.
- Aslam, J., Aslam, R., Alrefaee, S.H., Mobin, M., Aslam, A., Parveen, M., Hussain, C.M., 2020. Gravimetric, electrochemical, and morphological studies of an isoxazole derivative as corrosion inhibitor for mild steel in 1M HCl. *Arabian J. Chem.* 13, 7744–7758.
- Aslam, R., Mobin, M., Aslam, J., Lgaz, H., Chung, I.-M., 2019. Inhibitory effect of sodium carboxymethylcellulose and synergistic biodegradable gemini surfactants as effective inhibitors for MS corrosion in 1 M HCl. *J. Mater. Res. Technol.* 8, 4521–4533. <https://doi.org/10.1016/j.jmrt.2019.07.065>.
- Azzaoui, K., Mejdoubi, E., Jodeh, S., Lamhamdi, A., Rodriguez-Castellón, E., Algarra, M., Zarrouk, A., Errich, A., Salghi, R., Lgaz, H., 2017. Eco friendly green inhibitor Gum Arabic (GA) for the corrosion control of mild steel in hydrochloric acid medium. *Corros. Sci.* 129, 70–81.
- Bahlakeh, G., Ramezanzadeh, B., Dehghani, A., Ramezanzadeh, M., 2019. Novel cost-effective and high-performance green inhibitor based on aqueous Peganum harmala seed extract for mild steel corrosion in HCl solution: Detailed experimental and electronic/atomic level computational explorations. *J. Mol. Liq.* 283, 174–195. <https://doi.org/10.1016/j.molliq.2019.03.086>.
- Bammou, L., Belkhaouda, M., Salghi, R., Benali, O., Zarrouk, A., Zarrok, H., Hammouti, B., 2014. Corrosion inhibition of steel in sulfuric acidic solution by the chenopodium ambrosioides extracts. *J. Assoc. Arab Universities Basic Appl. Sci.* 16, 83–90. <https://doi.org/10.1016/j.jaubas.2013.11.001>.
- Benabbouha, T., Siniti, M., El Attari, H., Chefira, K., Chibi, F., Nmila, R., Rchid, H., 2018. Red Algae *Halopitys incurvus* extract as a green corrosion inhibitor of carbon steel in hydrochloric acid. *J. Bio-and Tribo-Corrosion* 4, 1–9.
- Benahmed, M., Selatnia, I., Djeddi, N., Akkal, S., Laouer, H., 2020. Adsorption and corrosion inhibition properties of butanolic extract of *Elaeoselinum thapsioides* and its synergistic effect with *Reutera lutea* (Desf.) Maires (Apiaceae) on A283 carbon steel in hydrochloric acid solution. *Chem. Africa* 3, 251–261. <https://doi.org/10.1007/s42250-019-00093-8>.
- Bhagavathula, A.S., Al-Khatib, A.J.M., Elnour, A.A., Al Kalbani, N. M., Shehab, A., 2015. *Ammi Visnaga* in treatment of urolithiasis and hypertriglyceridemia. *Pharmacognosy Res.* 7, 397.
- Bishr, M., El-Degwy, M., Hady, M.A., Amin, M., Salama, O., 2018. Supercritical fluid extraction of γ -Pyrone from *Ammi visnaga* L. fruits. *Future J. Pharm. Sci.* 4, 57–62.
- Bouknaana, D., Hammouti, B., Jodeh, S., Bouyanzer, A., Aouniti, A., Warad, I., 2015. Aqueous extracts of olive roots, stems, and leaves as eco-friendly corrosion inhibitor for steel in 1 M HCl medium. *Int. J. Ind. Chem.* 6, 233–245.
- Boulhaoua, M., El Hafi, M., Zehra, S., Eddaif, L., Alrashdi, A.A., Lahmidi, S., Guo, L., Mague, J.T., Lgaz, H., 2021. Synthesis, structural analysis and corrosion inhibition application of a new indazole derivative on mild steel surface in acidic media complemented with DFT and MD studies. *Colloids Surf. A* 617, <https://doi.org/10.1016/j.colsurfa.2021.126373> 126373.
- Brezinski, M.M., 1999. New Environmental Options for Corrosion Inhibitor Intensifiers. Presented at the SPE/EPA Exploration and Production Environment Conference, OnePetro. <https://doi.org/10.2118/52707-MS>.
- Chen, S., Chen, S., Zhu, B., Huang, C., Li, W., 2020. Magnolia grandiflora leaves extract as a novel environmentally friendly inhibitor for Q235 steel corrosion in 1 M HCl: Combining experimental and theoretical researches. *J. Mol. Liq.* 311, 113312.
- Chraka, A., Raissouni, I., Benseddik, N., Khayar, S., Mansour, A.I., Belcadi, H., Chaouket, F., Bouchta, D., 2020. Aging time effect of *Ammi visnaga* (L.) lam essential oil on the chemical composition and corrosion inhibition of brass in 3% NaCl medium. *Experimental and theoretical studies. Mater. Today: Proc.* 22, 83–88.
- Damej, M., Benmessaoud, M., Zehra, S., Kaya, S., Lgaz, H., Molhi, A., Labjar, N., El Hajjaji, S., Alrashdi, A.A., Lee, H.-S., 2021. Experimental and theoretical explorations of S-alkylated mercapto-benzimidazole derivatives for use as corrosion inhibitors for carbon steel in HCl. *J. Mol. Liq.* 331, <https://doi.org/10.1016/j.molliq.2021.115708> 115708.
- Dehghani, A., Bahlakeh, G., Ramezanzadeh, B., 2020a. Designing a novel targeted-release nano-container based on the silanized graphene oxide decorated with cerium acetylacetonate loaded beta-cyclodextrin (β -CD-CeA-MGO) for epoxy anti-corrosion coating. *Chem. Eng. J.* 400, <https://doi.org/10.1016/j.cej.2020.125860> 125860.
- Dehghani, A., Bahlakeh, G., Ramezanzadeh, B., 2019a. Green Eucalyptus leaf extract: a potent source of bio-active corrosion inhibitors for mild steel. *Bioelectrochemistry* 130, 107339.
- Dehghani, A., Bahlakeh, G., Ramezanzadeh, B., Ramezanzadeh, M., 2020b. Experimental complemented with microscopic (electronic/atomic)-level modeling explorations of *Laurus nobilis* extract as green inhibitor for carbon steel in acidic solution. *J. Ind. Eng. Chem.* 84, 52–71. <https://doi.org/10.1016/j.jiec.2019.12.019>.
- Dehghani, A., Bahlakeh, G., Ramezanzadeh, B., Ramezanzadeh, M., 2020c. Integrated modeling and electrochemical study of *Myrobalan* extract for mild steel corrosion retardation in acidizing media. *J. Mol. Liq.* 298, <https://doi.org/10.1016/j.molliq.2019.112046> 112046.
- Dehghani, A., Bahlakeh, G., Ramezanzadeh, B., Ramezanzadeh, M., 2019b. A combined experimental and theoretical study of green corrosion inhibition of mild steel in HCl solution by aqueous *Citrullus lanatus* fruit (CLF) extract. *J. Mol. Liq.* 279, 603–624. <https://doi.org/10.1016/j.molliq.2019.02.010>.
- Dutta, A., Saha, S.K., Adhikari, U., Banerjee, P., Sukul, D., 2017. Effect of substitution on corrosion inhibition properties of 2-(substituted phenyl) benzimidazole derivatives on mild steel in 1M HCl solution: A combined experimental and theoretical approach. *Corros. Sci.* 123, 256–266. <https://doi.org/10.1016/j.corsci.2017.04.017>.

- El Aoufir, Y., Aslam, R., Lazrak, F., Marzouki, R., Kaya, S., Skal, S., Ghanimi, A., Ali, I.H., Guenbour, A., Lgaz, H., Chung, I.-M., 2020. The effect of the alkyl chain length on corrosion inhibition performances of 1,2,4-triazole-based compounds for mild steel in 1.0 M HCl: Insights from experimental and theoretical studies. *J. Mol. Liq.* 303,. <https://doi.org/10.1016/j.molliq.2020.112631>
- Fan, B., Liu, Z., Zhao, X., Liu, H., Fan, G., Hao, H., 2021. Fabrication, characterization and efficient surface protection mechanism of poly (trans-cinnamaldehyde) electropolymerized coatings for EH36 steel in simulated seawater. *Colloids Surf. A* 629, 127434.
- Fan, B., Ma, Y., Wang, M., Hao, H., Yang, B., Lv, J., Sun, H., 2019. Revealing the assembly mechanism of an octadecylamine based supramolecular complex on mild steel in condensate water: correlative experimental and theoretical studies. *J. Mol. Liq.* 292, 111446.
- Fan, G., Liu, H., Fan, B., Ma, Y., Hao, H., Yang, B., 2020. Trazodone as an efficient corrosion inhibitor for carbon steel in acidic and neutral chloride-containing media: Facile synthesis, experimental and theoretical evaluations. *J. Mol. Liq.* 311, 113302.
- Farhadian, A., Rahimi, A., Safaei, N., Shaabani, A., Abdouss, M., Alavi, A., 2020. A theoretical and experimental study of castor oil-based inhibitor for corrosion inhibition of mild steel in acidic medium at elevated temperatures. *Corros. Sci.* 175, 108871.
- Fouda, A., Hegazi, M., El-Azaly, A., 2019. Henna extract as green corrosion inhibitor for carbon steel in hydrochloric acid solution. *Int. J. Electrochem. Sci.* 14, 4668–4682.
- Fouda, A.-E.-A.-S., Nazeer, A.A., Ibrahim, M., Fakih, M., 2013. Ginger extract as green corrosion inhibitor for steel in sulfide polluted salt water. *J. Korean Chem. Soc.* 57, 272–278.
- Franchi, G.G., Bovalini, L., Martelli, P., Ferri, S., Sbardellati, E., 1985. High performance liquid chromatography analysis of the furanochromones khellin and visnagin in various organs of Ammi visnaga (L.) Lam. at different developmental stages. *J. Ethnopharmacol.* 14, 203–212.
- Furtado, L.B., Nascimento, R., Seidl, P.R., Guimaraes, M.J.O., Costa, L.M., Rocha, J., Ponciano, J., 2019. Eco-friendly corrosion inhibitors based on Cashew nut shell liquid (CNSL) for acidizing fluids. *J. Mol. Liq.* 284, 393–404.
- Gadow, H., Motawea, M., 2017. Investigation of the corrosion inhibition of carbon steel in hydrochloric acid solution by using ginger roots extract. *RSC Adv.* 7, 24576–24588.
- Günaydn, K., Erim, F.B., 2002. Determination of khellin and visnagin in Ammi visnaga fruits by capillary electrophoresis. *J. Chromatogr. A* 954, 291–294.
- Guo, L., Bakri, Y.E., Yu, R., Tan, J., Essassi, E.M., 2020. Newly synthesized triazolopyrimidine derivative as an inhibitor for mild steel corrosion in HCl medium: an experimental and in silico study. *J. Mater. Res. Technol.* 9, 6568–6578. <https://doi.org/10.1016/j.jmrt.2020.04.044>
- Hanini, K., Merzoug, B., Boudiba, S., Selatnia, I., Laouer, H., Akkal, S., 2019. Influence of different polyphenol extracts of *Taxus baccata* on the corrosion process and their effect as additives in electrodeposition. *Sustainable Chem. Pharm.* 14,. <https://doi.org/10.1016/j.scp.2019.100189>
- Haque, J., Srivastava, V., Chauhan, D.S., Lgaz, H., Quraishi, M.A., 2018. Microwave-induced synthesis of chitosan Schiff bases and their application as novel and green corrosion inhibitors: experimental and theoretical approach. *ACS Omega* 3, 5654–5668. <https://doi.org/10.1021/acsomega.8b00455>
- Harb, M.B., Abubshait, S., Eteyeb, N., Kamoun, M., Dhoubi, A., 2020. Olive leaf extract as a green corrosion inhibitor of reinforced concrete contaminated with seawater. *Arabian J. Chem.* 13, 4846–4856.
- Hemapriya, V., Prabakaran, M., Chitra, S., Swathika, M., Kim, S.-H., Chung, I.-M., 2020. Utilization of biowaste as an eco-friendly biodegradable corrosion inhibitor for mild steel in 1 mol/L HCl solution. *Arabian J. Chem.* 13, 8684–8696. <https://doi.org/10.1016/j.arabj.2020.09.060>
- Hoai, N.T., Van Hien, P., Vu, N.S.H., Son, D.L., Van Man, T., Tri, M.D., Nam, N.D., 2019. An improved corrosion resistance of steel in hydrochloric acid solution using Hibiscus sabdariffa leaf extract. *Chem. Pap.* 73, 909–925.
- Ikpeseni, S.C., Odu, G.O., Owamah, H.I., Onochie, P.U., Ukala, D. C., 2021. Thermodynamic parameters and adsorption mechanism of corrosion inhibition in mild steel using jatropha leaf extract in hydrochloric acid. *Arabian Journal for Science and Engineering*, 1–11.
- Ishak, A., Adams, F.V., Madu, J.O., Joseph, I.V., Olubambi, P.A., 2019. Corrosion Inhibition of Mild Steel in 1M Hydrochloric Acid using Haematostaphis barteri Leaves Extract. *Procedia Manufacturing*, The 2nd International Conference on Sustainable Materials Processing and Manufacturing, SMPM 2019, 8-10 March 2019, Sun City, South Africa 35, 1279–1285. [10.1016/j.promfg.2019.06.088](https://doi.org/10.1016/j.promfg.2019.06.088)
- Jafari, H., Akbarzade, K., Danaee, I., 2019. Corrosion inhibition of carbon steel immersed in a 1M HCl solution using benzothiazole derivatives. *Arabian J. Chem.* 12, 1387–1394. <https://doi.org/10.1016/j.arabj.2014.11.018>
- Jensen, W.B., 2007. The origin of the Soxhlet extractor. *J. Chem. Educ.* 84, 1913.
- Kadiri, L., Galai, M., Ouakki, M., Essaadaoui, Y., Ouass, A., Cherkaoui, M., Rifi, E.-H., Lebkiri, A., 2018. Coriandrum Sativum. L seeds extract as a novel green corrosion inhibitor for mild steel in 1.0 M hydrochloric and 0.5 M sulfuric solutions. *Anal. Bioanal. Chem.* 10, 249–268.
- Khadraoui, A., Khelifa, A., Hamitouche, H., Mehdaoui, R., 2014. Inhibitive effect by extract of *Mentha rotundifolia* leaves on the corrosion of steel in 1 M HCl solution. *Res. Chem. Intermed.* 40, 961–972.
- Khalaf, M.M., Tantawy, A.H., Soliman, K.A., Abd El-Lateef, H.M., 2020. Cationic gemini-surfactants based on waste cooking oil as new 'green' inhibitors for N80-steel corrosion in sulphuric acid: a combined empirical and theoretical approaches. *J. Mol. Struct.* 1203, 127442.
- Koch, G., Varney, J., Thompson, N., Moghissi, O., Gould, M., Payer, J., 2016. International measures of prevention, application, and economics of corrosion technologies study. *NACE international* 216.
- Kumar, D., Jain, N., Jain, V., Rai, B., 2020. Amino acids as copper corrosion inhibitors: A density functional theory approach. *Appl. Surf. Sci.* 514,. <https://doi.org/10.1016/j.apsusc.2020.145905>
- Laamari, R., Benzakour, J., Berrekhis, F., Abouelfida, A., Derja, A., Villemin, D., 2011. Corrosion inhibition of carbon steel in hydrochloric acid 0.5M by hexa methylene diamine tetramethylphosphonic acid. *Arabian J. Chem.* 4, 271–277. <https://doi.org/10.1016/j.arabj.2010.06.046>
- Larabi, L., Harek, Y., Traisnel, M., Mansri, A., 2004. Synergistic influence of poly(4-vinylpyridine) and potassium iodide on inhibition of corrosion of mild steel in 1M HCl. *J. Appl. Electrochem.* 34, 833–839. <https://doi.org/10.1023/B:JACH.0000035609.09564.e6>
- Lgaz, H., Chung, I.-M., Albayati, M.R., Chaoui, A., Salghi, R., Mohamed, S.K., 2020a. Improved corrosion resistance of mild steel in acidic solution by hydrazone derivatives: An experimental and computational study. *Arabian J. Chem.* 13, 2934–2954. <https://doi.org/10.1016/j.arabj.2018.08.004>
- Lgaz, H., Saha, S.Kr., Chaoui, A., Bhat, K.S., Salghi, R., Shubhalaxmi, Banerjee, P., Ali, I.H., Khan, M.I., Chung, I.-M., 2020b. Exploring the potential role of pyrazoline derivatives in corrosion inhibition of mild steel in hydrochloric acid solution: Insights from experimental and computational studies. *Construction and Building Materials* 233, 117320. [10.1016/j.conbuildmat.2019.117320](https://doi.org/10.1016/j.conbuildmat.2019.117320)
- Liu, H., Fan, B., Fan, G., Ma, Y., Hao, H., Zhang, W., 2021a. Anti-corrosive mechanism of poly (N-ethylaniline)/sodium silicate elec-

- trochemical composites for copper: Correlated experimental and in-silico studies. *J. Mater. Sci. Technol.* 72, 202–216.
- Liu, H., Fan, B., Fan, G., Zhao, X., Liu, Z., Hao, H., Yang, B., 2021b. Long-term protective mechanism of poly (N-methylaniline)/phosphate one-step electropolymerized coatings for copper in 3.5% NaCl solution. *J. Alloy. Compd.* 872, 159752.
- Liu, Y., Song, Z., Wang, W., Jiang, L., Zhang, Y., Guo, M., Song, F., Xu, N., 2019. Effect of ginger extract as green inhibitor on chloride-induced corrosion of carbon steel in simulated concrete pore solutions. *J. Cleaner Prod.* 214, 298–307.
- Loganayagi, C., Kamal, C., Sethuraman, M., 2014. Opuntia: An active principle of *Opuntia elatior* as an eco-friendly inhibitor of corrosion of mild steel in acid medium. *ACS Sustainable Chem. Eng.* 2, 606–613.
- Ma, Y., Zhou, T., Zhu, W., Fan, B., Liu, H., Fan, G., Hao, H., Sun, H., Yang, B., 2020. Understanding the anticorrosive mechanism of a cross-linked supramolecular polymer for mild steel in the condensate water: comprehensive experimental, molecular docking, and molecular dynamics investigations. *J. Mol. Model.* 26, 1–17.
- Majd, M.T., Asaldoust, S., Bahlakeh, G., Ramezanzadeh, B., Ramezanzadeh, M., 2019. Green method of carbon steel effective corrosion mitigation in 1 M HCl medium protected by *Primula vulgaris* flower aqueous extract via experimental, atomic-level MC/MD simulation and electronic-level DFT theoretical elucidation. *J. Mol. Liq.* 284, 658–674.
- Meng, S., Liu, Z., Zhao, X., Fan, B., Liu, H., Guo, M., Hao, H., 2021. Efficient corrosion inhibition by sugarcane purple rind extract for carbon steel in HCl solution: mechanism analyses by experimental and in silico insights. *RSC Adv.* 11, 31693–31711.
- Metals, A.C.G.-1 on C. of, 2017. Standard practice for preparing, cleaning, and evaluating corrosion test specimens. ASTM international.
- Mizuno, A., Takata, M., Okada, Y., Okuyama, T., Nishino, H., Nishino, A., Takayasu, J., Iwashima, A., 1994. Structures of New Coumarins and Antitumor-Promoting Activity of Coumarins from *Angelica edulis*. *Planta Med.* 60, 333–336.
- Mobin, M., Ahmad, I., Basik, M., Murmu, M., Banerjee, P., 2020. Experimental and theoretical assessment of almond gum as an economically and environmentally viable corrosion inhibitor for mild steel in 1 M HCl. *Sustainable Chem. Pharm.* 18. <https://doi.org/10.1016/j.scp.2020.100337>.
- Mobin, M., Aslam, R., Zehra, S., Ahmad, M., 2017. Bio/environment-friendly cationic gemini surfactant as novel corrosion inhibitor for mild steel in 1 M HCl solution. *J. Surfactants Deterg.* 20, 57–74.
- Mobin, M., Basik, M., Aslam, J., 2019a. Pineapple stem extract (Bromelain) as an environmental friendly novel corrosion inhibitor for low carbon steel in 1 M HCl. *Measurement* 134, 595–605.
- Mobin, M., Basik, M., El Aoufir, Y., 2019b. Corrosion mitigation of mild steel in acidic medium using *Lagerstroemia speciosa* leaf extract: A combined experimental and theoretical approach. *J. Mol. Liq.* 286, 110890.
- Mobin, M., Rizvi, M., 2017. Adsorption and corrosion inhibition behavior of hydroxyethyl cellulose and synergistic surfactants additives for carbon steel in 1M HCl. *Carbohydr. Polym.* 156, 202–214. <https://doi.org/10.1016/j.carbpol.2016.08.066>.
- Muthukumarasamy, K., Pitchai, S., Devarayan, K., Nallathambi, L., 2020. Adsorption and corrosion inhibition performance of *Tunbergia fragrans* extract on mild steel in acid medium. *Materials Today: Proceedings, International Conference on Nanotechnology: Ideas, Innovation and Industries* 33, 4054–4058. <https://doi.org/10.1016/j.matpr.2020.06.533>.
- Oguzie, E.E., Adindu, C.B., Enenebeaku, C.K., Ogukwe, C.E., Chidiebere, M.A., Oguzie, K.L., 2012. Natural products for materials protection: mechanism of corrosion inhibition of mild steel by acid extracts of *Piper guineense*. *The Journal of Physical Chemistry C* 116, 13603–13615.
- Olasunkanmi, L.O., Idris, A.O., Adewole, A.H., Wahab, O.O., Ebenso, E.E., 2020. Adsorption and Corrosion Inhibition Potentials of Salicylaldehyde-based Schiff Bases of Semicarbazide and p-Toluidine on Mild Steel in Acidic Medium: Experimental and Computational Studies. *Surf. Interfaces* 21. <https://doi.org/10.1016/j.surf.2020.100782>.
- Orazem, M.E., Tribollet, B., 2008. *Electrochemical impedance spectroscopy*. New Jersey, 383–389.
- Oyekunle, D.T., Oguntade, T.I., Ita, C.S., Ojo, T., Orodu, O.D., 2019. Corrosion inhibition of mild steel using binary mixture of sesame and castor oil in brine solution. *Mater. Today Commun.* 21, 100691.
- Palaniappan, N., Alphonsa, J., Cole, I.S., Balasubramanian, K., Bosco, I.G., 2019. Rapid investigation expiry drug green corrosion inhibitor on mild steel in NaCl medium. *Mater. Sci. Eng., B* 249, 114423.
- Poberžnik, M., Chiter, F., Milošev, I., Marcus, P., Costa, D., Kokalj, A., 2020. DFT study of n-alkyl carboxylic acids on oxidized aluminum surfaces: From standalone molecules to self-assembled-monolayers. *Appl. Surf. Sci.* 525. <https://doi.org/10.1016/j.apusc.2020.146156>.
- Pradityana, A., Shahab, A., Noerochim, L., Susanti, D., 2016. Inhibition of corrosion of carbon steel in 3.5% NaCl solution by *Myrmecodia Pendans* extract. *Int. J. Corrosion* 2016.
- Reynolds, M.A., 2020. A technical playbook for chemicals and additives used in the hydraulic fracturing of shales. *Energy Fuels* 34, 15106–15125.
- Saha, S.K., Dutta, A., Ghosh, P., Sukul, D., Banerjee, P., 2016a. Novel Schiff-base molecules as efficient corrosion inhibitors for mild steel surface in 1 M HCl medium: experimental and theoretical approach. *PCCP* 18, 17898–17911. <https://doi.org/10.1039/C6CP01993E>.
- Saha, S.K., Murmu, M., Murmu, N.C., Banerjee, P., 2016b. Evaluating electronic structure of quinazolinone and pyrimidinone molecules for its corrosion inhibition effectiveness on target specific mild steel in the acidic medium: a combined DFT and MD simulation study. *J. Mol. Liq.* 224, 629–638.
- Sanaei, Z., Ramezanzadeh, M., Bahlakeh, G., Ramezanzadeh, B., 2019. Use of *Rosa canina* fruit extract as a green corrosion inhibitor for mild steel in 1M HCl solution: A complementary experimental, molecular dynamics and quantum mechanics investigation. *J. Ind. Eng. Chem.* 69, 18–31. <https://doi.org/10.1016/j.jiec.2018.09.013>.
- Saxena, A., Prasad, D., Haldhar, R., Singh, G., Kumar, A., 2018. Use of *Sida cordifolia* extract as green corrosion inhibitor for mild steel in 0.5 M H₂SO₄. *J. Environ. Chem. Eng.* 6, 694–700. <https://doi.org/10.1016/j.jece.2017.12.064>.
- Sharma, S.K., Mudhoo, A., Jain, G., Khamis, E., 2009. Corrosion inhibition of Neem (*Azadirachta indica*) leaves extract as a green corrosion inhibitor for Zinc in H₂SO₄. *Green Chem. Lett. Rev.* 2, 47–51.
- Sharma, S.K., Peter, A., Obot, I.B., 2015. Potential of *Azadirachta indica* as a green corrosion inhibitor against mild steel, aluminum, and tin: a review. *J. Anal. Sci. Technol.* 6, 1–16.
- Shekhar, C., Jaiswal, A., Ji, G., Prakash, R., 2021. Ethanol extract of waste potato peels for corrosion inhibition of low carbon steel in chloride medium. *Mater. Today: Proc.* 44, 2267–2272.
- Solmaz, R., 2014a. Investigation of corrosion inhibition mechanism and stability of Vitamin B1 on mild steel in 0.5 M HCl solution. *Corros. Sci.* 81, 75–84. <https://doi.org/10.1016/j.corsci.2013.12.006>.
- Solmaz, R., 2014b. Investigation of adsorption and corrosion inhibition of mild steel in hydrochloric acid solution by 5-(4-Dimethylaminobenzylidene)rhodanine. *Corros. Sci.* 79, 169–176. <https://doi.org/10.1016/j.corsci.2013.11.001>.
- Srivastava, M., 2020. Mild Steel Corrosion Inhibition, in 4 N Sulphuric Acid, by a Green Inhibitor. *Portugaliae Electrochimica Acta* 38, 99–106.

- Verma, C., Alrefaee, S.H., Rhee, K.Y., Quraishi, M.A., Ebenso, E.E., 2021. Thiol (-SH) substituent as functional motif for effective corrosion protection: A review on current advancements and future directions. *J. Mol. Liq.* 324,. <https://doi.org/10.1016/j.molliq.2020.115111> 115111.
- Verma, C., Ebenso, E.E., Bahadur, I., Quraishi, M.A., 2018a. An overview on plant extracts as environmental sustainable and green corrosion inhibitors for metals and alloys in aggressive corrosive media. *J. Mol. Liq.* 266, 577–590. <https://doi.org/10.1016/j.molliq.2018.06.110>.
- Verma, C., Lgaz, H., Verma, D.K., Ebenso, E.E., Bahadur, I., Quraishi, M.A., 2018b. Molecular dynamics and Monte Carlo simulations as powerful tools for study of interfacial adsorption behavior of corrosion inhibitors in aqueous phase: A review. *J. Mol. Liq.* 260, 99–120. <https://doi.org/10.1016/j.molliq.2018.03.045>.
- Verma, C., Olasunkanmi, L.O., Ebenso, E.E., Quraishi, M.A., 2018c. Substituents effect on corrosion inhibition performance of organic compounds in aggressive ionic solutions: A review. *J. Mol. Liq.* 251, 100–118. <https://doi.org/10.1016/j.molliq.2017.12.055>.
- Verma, C., Olasunkanmi, L.O., Ebenso, E.E., Quraishi, M.A., Obot, I. B., 2016. Adsorption behavior of glucosamine-based, pyrimidine-fused heterocycles as green corrosion inhibitors for mild steel: experimental and theoretical studies. *J. Phys. Chem. C* 120, 11598–11611.
- Zaher, A., Chaouiki, A., Salghi, R., Boukhraz, A., Bourkhiss, B., Ouhssine, M., 2020. Inhibition of mild steel corrosion in 1M hydrochloric medium by the methanolic extract of Ammi Visnaga L. lam seeds. *Int. J. Corros.* 2020.
- Znini, M., Majidi, L., Bouyanzer, A., Paolini, J., Desjobert, J.M., Costa, J., Hammouti, B., 2012. Essential oil of *Salvia aucheri* mesatlantica as a green inhibitor for the corrosion of steel in 0.5M H 2SO 4. *Arabian J. Chem.* 5, 467–474. <https://doi.org/10.1016/j.arabjc.2010.09.017>.